Resonant tunneling through double-barrier structures on graphene*

Deng Wei-Yin(邓伟胤)[a], Zhu Rui(朱 瑞)[a], Xiao Yun-Chang(肖运昌)[b], and Deng Wen-Ji(邓文基)[a]†

[a] *Department of Physics, South China University of Technology, Guangzhou* 510640, *China*
[b] *LQIT, ICMP and SPTE, South China Normal University, Guangzhou* 510006, *China*

(Received 5 July 2013; revised manuscript received 6 August 2013; published 3 December 2013)

Quantum resonant tunneling behaviors of double-barrier structures on graphene are investigated under the tight-binding approximation. The Klein tunneling and resonant tunneling are demonstrated for the quasiparticles with energy close to the Dirac points. The Klein tunneling vanishes by increasing the height of the potential barriers to more than 300 meV. The Dirac transport properties continuously change to the Schrödinger ones. It is found that the peaks of resonant tunneling approximate to the eigen-levels of graphene nanoribbons under appropriate boundary conditions. A comparison between the zigzag- and armchair-edge barriers is given.

Keywords: graphene, tight-binding approximation, resonant tunneling

PACS: 72.80.Vp, 73.23.Ad, 73.40.Gk **DOI:** 10.1088/1674-1056/23/1/017202

1. Introduction

In recent years, the physical properties of graphene have been extensively studied both theoretically and experimentally.[1–3] The low-energy electronic states in graphene can be described by the Dirac equation, while their high-energy counterparts obey the usual Schrödinger physics. Because of the linear dispersion relation at low energies, many unusual physical behaviors have been found, such as the Klein paradox,[4] the conductance minimum,[5] the unconventional quantum Hall effect,[6–8] the shot noise with a Fano factor close to $1/3$,[9–11] the sign reverse in quantum pumping[12–14] and the specular Andreev reflection in a superconductor junction.[15–19] Based on these extraordinary properties, graphene has many potential applications, such as transistors,[20,21] strain sensors,[22] electrodes[23] and entanglement sources.[24,25]

One of the proposed devices is the graphene-based single- and multi-potential-barrier structures.[26–31] Katsnelson *et al.* calculated the resonant condition of transmission in a single-barrier system and found that the resonant Fermi energy satisfies $E = V_0 \pm [(N\pi/d)^2 + k_y^2]^{1/2}$, where $N = 0, \pm 1, \ldots$ and V_0 is the height of the barrier.[4] Bai *et al.* studied the transport properties in graphene superlattices and found that the normal-incidence transmission resonances occur in the bilayer graphene structure but not in the monolayer one as a result of the Klein paradox.[26] The resonant tunneling through graphene-based double barriers has been studied by Pereira *et al.*; they analyzed the origin of the resonance effect in the system and found that the resonant features result from the resonant electron states in the wells or the hole states in the barriers.[27] However, most of the previous works focused on the low-energy Dirac regime and left the high-energy Schrödinger regime and that in between untouched.

In this paper, we revisit the resonant tunneling processes in the graphene-based double-barrier structure. The tight-binding approach we used works in the whole energy regime beyond the low-energy Dirac equation approximation. The previous published results can be recovered. However, we mainly focus on the regime where the potentials are so strong that in the barrier regions, the electronic states cannot be described by the Dirac equation. A continuous transition from the Klein tunneling is also discussed. So we consider a hybrid system in which the electronic states are described by the Dirac equation in the non-barrier regions and they are described by both the Schrödinger and the Dirac equations in the barrier regions depending on the barrier heights.

2. Model and formulation

We consider the double-barrier model in an undoped graphene sheet occupying the x–y plane, in which the left and right parts are two semi-infinite leads separated by the electric gates' modulated region. The geometry sketch is shown in Fig. 1. The grown direction is taken as the x axis and the width along the y direction is infinite. The left lead extends from $x = -\infty$ to $x = n_1 l$, where $l = \sqrt{3}a_0/2$ and the lattice constant[32] is $a_0 = 0.246$ nm. The left barrier region contains $N_1 = n_2 - n_1$ zigzag chains so the width of this region is $N_1 l$; and the right barrier region contains $N_2 = n_4 - n_3$ zigzag chains; the middle region contains $M = n_3 - n_2$ zigzag chains so its width is Ml; and the right lead occupies $x > n_4 l$.

*Project supported by the National Natural Science Foundation of China (Grant No. 11004063) and the Fundamental Research Funds for the Central Universities, China (Grant No. 2012ZZ0076).

†Corresponding author. E-mail: phwjdeng@scut.edu.cn

© 2014 Chinese Physical Society and IOP Publishing Ltd

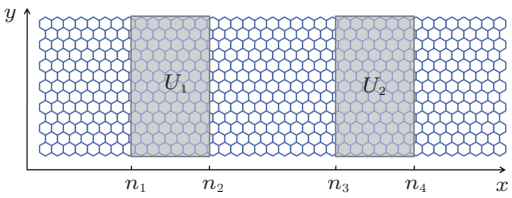


Fig. 1. (color online) Sketch of the double-barrier structure in graphene.

According to the tight-binding approximation, the corresponding Schrödinger equation is

$$\varepsilon_n \varphi_n + \sum_{\delta} t_{n,n+\delta} \varphi_{n+\delta} = E \varphi_n, \tag{1}$$

where subscript n is the ordinal number of the atoms, φ_n denotes the wave function in the Wannier representation and ε_n and $t_{n,n+\delta}$ denote the site energy and the nearest-neighbor hopping integral, respectively. In perfect graphene, the structure is composed of two sublattices labeled by A and B. In the presence of a one-dimensional (1D) confining potential $U = U(x)$, the lattice wave function can be written as $\varphi^{\mathrm{A,B}}_{n,m-1} = \mathrm{e}^{-\mathrm{i}a_0 k_y} \varphi^{\mathrm{A,B}}_{n,m}$ due to the translational invariance along the y direction. Substituting it into Eq. (1), we have

$$\begin{aligned} -\psi^{\mathrm{A}}_{n-1} + (\varepsilon_n - E)\, \psi^{\mathrm{B}}_n - \tau \psi^{\mathrm{A}}_n = 0, \\ -\tau \psi^{\mathrm{B}}_n + (\varepsilon_n - E)\, \psi^{\mathrm{A}}_n - \psi^{\mathrm{B}}_{n+1} = 0, \end{aligned} \tag{2}$$

where $\psi^{\mathrm{B}}_n = \varphi^{\mathrm{B}}_{n,m}$, $\psi^{\mathrm{B}}_{n+1} = \mathrm{e}^{\mathrm{i}a_0 k_y/2} \varphi^{\mathrm{B}}_{n+1,m}$, $\psi^{\mathrm{A}}_n = \mathrm{e}^{\mathrm{i}a_0 k_y/2} \varphi^{\mathrm{A}}_{n,m}$, $\psi^{\mathrm{A}}_{n+1} = \varphi^{\mathrm{A}}_{n+1,m}$, and $\tau = 2t_0 \cos(a_0 k_y/2)$. The gated site energies can be written as

$$\begin{aligned} \varepsilon^{\mathrm{B}}_n &= \begin{cases} \varepsilon_0 + U_1, & n_1 < n \le n_2, \\ \varepsilon_0, & \text{others}, \\ \varepsilon_0 + U_2, & n_3 < n \le n_4, \end{cases} \\ \varepsilon^{\mathrm{A}}_n &= \begin{cases} \varepsilon_0 + U_1, & n_1 \le n < n_2, \\ \varepsilon_0, & \text{others}, \\ \varepsilon_0 + U_2. & n_3 \le n < n_4. \end{cases} \end{aligned} \tag{3}$$

We define the dimensionless variables $U_j \to U_j/t_0$ and $x \to x/l$ and set the site energy of the gate-free regions to be $\varepsilon_0 = 0$. The homogeneous hopping integrals are $t_{n,n+\delta} = -t_0 = -2.7$ eV. Hence the solution of incidence from the left reservoir can be written as

$$\psi^{\mathrm{B}}_n = \begin{cases} \mathrm{e}^{\mathrm{i}\kappa(n-n_1)} + r\mathrm{e}^{-\mathrm{i}\kappa(n-n_1)}, & n \le n_1, \\ A_2 \mathrm{e}^{\mathrm{i}\kappa_1(n-n_1)} + B_2 \mathrm{e}^{-\mathrm{i}\kappa_1(n-n_1)}, & n_1 < n \le n_2, \\ A_3 \mathrm{e}^{\mathrm{i}\kappa(n-n_2)} + B_3 \mathrm{e}^{-\mathrm{i}\kappa(n-n_2)}, & n_2 < n \le n_3, \\ A_4 \mathrm{e}^{\mathrm{i}\kappa_2(n-n_3)} + B_4 \mathrm{e}^{-\mathrm{i}\kappa_2(n-n_3)}, & n_3 < n \le n_4, \\ t\,\mathrm{e}^{\mathrm{i}\kappa(n-n_4)}, & n > n_4, \end{cases} \tag{4}$$

$$\psi^{\mathrm{A}}_n = \begin{cases} a\mathrm{e}^{\mathrm{i}\kappa(n-n_1)} + a^* r \mathrm{e}^{-\mathrm{i}\kappa(n-n_1)}, & n < n_1, \\ a_{1+} A_2 \mathrm{e}^{\mathrm{i}\kappa_1(n-n_1)} + a_{1-} B_2 \mathrm{e}^{-\mathrm{i}\kappa_1(n-n_1)}, & n_1 \le n < n_2, \\ a A_3 \mathrm{e}^{\mathrm{i}\kappa(n-n_2)} + a^* B_3 \mathrm{e}^{-\mathrm{i}\kappa(n-n_2)}, & n_2 \le n < n_3, \\ a_{2+} A_4 \mathrm{e}^{\mathrm{i}\kappa_2(n-n_3)} + a_{2-} B_4 \mathrm{e}^{-\mathrm{i}\kappa_2(n-n_3)}, & n_3 \le n < n_4, \\ a t \mathrm{e}^{\mathrm{i}\kappa(n-n_4)}, & n \ge n_4, \end{cases} \tag{5}$$

where κ, κ_1, κ_2 are the dimensionless momenta along the x direction in the normal, left-barrier and right-barrier regions, respectively. They are determined by the dispersion relations

$$\begin{aligned} E &= \pm \left| \tau + \mathrm{e}^{\mathrm{i}\kappa} \right|, \\ E &= U_1 \pm \sqrt{\tau^2 + \tau\left(\mathrm{e}^{\mathrm{i}\kappa_1} + \mathrm{e}^{-\mathrm{i}\kappa_1}\right) + 1}, \\ E &= U_2 \pm \sqrt{\tau^2 + \tau\left(\mathrm{e}^{\mathrm{i}\kappa_2} + \mathrm{e}^{-\mathrm{i}\kappa_2}\right) + 1}. \end{aligned} \tag{6}$$

Here, $a = -(\tau + \mathrm{e}^{\mathrm{i}\kappa})/E$, $a_{1\pm,2\pm} = -(\tau + \mathrm{e}^{\pm\mathrm{i}\kappa_{1,2}})/(\varepsilon - U_{1,2})$, a^* is the complex conjugate of a; A_i, B_i $(i = 2,3,4)$ are the amplitudes of the wave functions traveling along the x and $-x$ directions of the i-th region. Then r and t are the reflection and transmission amplitudes, respectively, which can be determined by matching the eigen equations at the region interfaces.

By comparing with the *ab initio* calculation, we know that the nearest-neighbor tight-binding model in graphene is valid at energies below 2 eV,[32] which is much higher than the energy of Dirac-like particles (< 1 eV,[4] actually, the energy should be less than 300 meV, as discussed below). We choose the $\boldsymbol{K}$ point ($\boldsymbol{K} = 2\pi(0, 2/3)/a_0$) as the origin and the incident angle θ spans between k_x and k_y. When the Fermi energy agrees with the allowed energy of the structure, the resonance effect occurs. The resonance effect in this structure includes the quasiparticle resonance in the barriers, the resonance in the middle region and the hybridization between them. When the Fermi energy is in the barrier, the resonance comes from the hole eigen-states, while it comes from the electron ones in the middle region. In our model, the barriers and the middle regions are infinite-length zigzag nanoribbons. The edge state energy is very small compared to the Fermi energy when the nanoribbon is wide enough, so it does not reshape the resonance effect. The dispersion of the standing wave state in the zigzag nanoribbon[33] is

$$\varepsilon_{\pm} = \pm \left| 1 + \tau \mathrm{e}^{\mathrm{i}\kappa} \right|, \tag{7}$$

and the wave vector can be determined from the relation

$$\frac{1 + \tau \mathrm{e}^{\mathrm{i}\kappa}}{\left| 1 + \tau \mathrm{e}^{\mathrm{i}\kappa} \right|} \mathrm{e}^{\mathrm{i}M\kappa} = \pm 1, \tag{8}$$

where M is the width of the nanoribbon. When the Fermi energy is equal to one of the allowed energies in the zigzag nanoribbon, namely $E = \varepsilon_{\pm}$, the resonance effect occurs. For the normal accidence, $\tau = -1$ and $\kappa = \pi(1 + 2n)/(2M + 1)$, $n = 1, 2, \ldots, M$. When the incident energy is small or M is very large, κ is small. Eigen energies (7) can be approximated as

$$\varepsilon_{\pm} = \pm [2(1 - \cos\kappa)]^{1/2} \approx \pm\kappa \approx \pm \left(n + \frac{1}{2} \right) \frac{\pi}{M}. \tag{9}$$

The separation between two transmission resonances is π/M. It is difficult to obtain an analytical expression of the allowed

energies for large incident angles because of the anisotropic momentum space. If the barriers and the middle regions are Armchair nanoribbons along the x direction, the resonance energy is a little different from that of the above system. In this case, the vector in the confined direction $k_y = [\sqrt{3}n\pi/(M+1)+2\pi/\sqrt{3}]$ is not related to vector κ in the infinite direction.[34,35] The first order approximate allowed energy of the Taylor expansion is zero; the second one can be obtained as

$$\varepsilon_{\pm} \approx \pm\sqrt{\left(\frac{\sqrt{3}n\pi}{M+1}\right)^2+\kappa^2}, \tag{10}$$

where $(M+1)/\sqrt{3}$ is the dimensionless width of the Armchair nanoribbon. This is the same as the resonance condition of the low energy situation because of the similar structure of the momentum space where the vectors of the two directions are independent.[4]

With the obtained transmission coefficients, the Landauer–Büttiker conductance can be calculated as[36–38]

$$G(E_{\rm F}) = G_0\int_{-\pi/2}^{\pi/2} T(E_{\rm F}, k_{\rm F}\sin\theta)\cos\theta\,{\rm d}\theta, \tag{11}$$

where θ is the incident angle relative to the x direction, $G_0 = 2e^2k_{\rm F}L_y/(\pi h)$ is taken as the conductance unit, L_y is the sample size along the y direction and $k_{\rm F} = \sqrt{\kappa^2+k_y^2}$.

3. Numerical results and discussion

In the numerical calculations, we take $U_1 = U_2 = U$. The transmission $T(E,\theta,U,N_1,M,N_2)$ and conductance G are functions of the Fermi energy, the incident angle, the strength of the double potentials and the widths of the barriers and the middle regions.

We calculate the transmission as a function of the Fermi energy for different N_j $(j=1,2)$ and M at normal incidence $(\theta=0)$, as shown in Fig. 2. The black dotted line, blue dashed line and red solid line correspond to $(N_1,M,N_2) = (468,0,0)$, $(25,200,20)$ and $(468,200,468)$, respectively. From Fig. 2, we find three noteworthy features. First, there is no Klein tunneling with perfect transmission at all energies in the normal incidence. The potentials are so high that the Dirac equation is not satisfied in the barrier regions. Second, for $(N_1,M,N_2) = (468,0,0)$ or $(25,200,20)$, the separation between neighbored transmission resonance peaks is equal, which can be seen in Eq. (9). This is different from the resonance effect in the free electron gas, which has the n^2 relation to the incident energy. Third, the resonance effect in this system includes the resonance in the barriers, the resonance in the middle region and the hybridization between them. This property is nontrivial since the resonance in the barriers is a result of hole quasibound levels, which does not occur in semiconductor superlattices with band gaps forming the potential barriers. For $(N_1,M,N_2) = (468,0,0)$, the resonance effect is in the single barrier; for $(N_1,M,N_2) = (25,200,20)$, the resonance effect is in the middle region. The width of the barriers is so small and the bound level interval is so large that the resonance effect in the barriers is invisible in the energy range shown in the figure and the unequal widths can suppress the resonance effect more. For $(N_1,M,N_2) = (468,200,468)$, the resonance peaks contain contributions from the quasibound states in the barriers as well as in the middle region. The extra resonance peaks are the hybridization of the three regions.

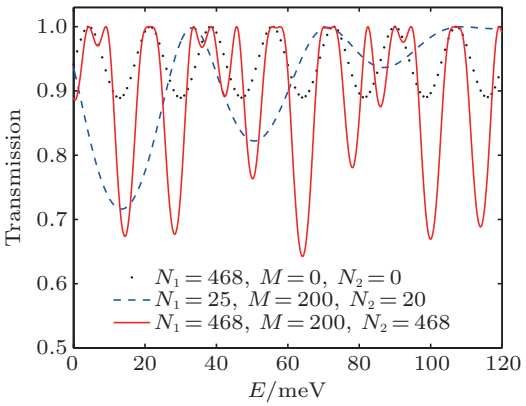


Fig. 2. (color online) Transmission probability of normal incidence as a function of the Fermi energy. The potential strength is $U = 1800$ meV.

Figure 3 shows the transmission as a function of the incident angle for different Fermi energies, $E = 75$ meV, 35 meV, 30 meV, 15 meV, corresponding to red solid, blue dashed, green dash-dotted and black dotted lines, respectively. All of the four lines demonstrate the same feature of incident-angle asymmetry. This can be intuitively understood from the dispersion relation of infinite graphene around the $\boldsymbol{K}$ point. The energy is asymmetric about k_x for large quasiparticle energies when the dispersion relation is not linear. Then the wave vector of angle θ is different from that of angle $-\theta$ at the same incident energy. This leads to the asymmetry of transmission about the incident angle. Among the four lines, the other shared feature is that the perfect transmission occurs at some particular incident angles as a result of the resonance effect.[27] At these incident angles, the Fermi energy is equal to the allowed energy of one of the zigzag nanoribbons. In addition, the resonant peak number increases with the increasing Fermi energy.

In Fig. 4, the normal-incidence transmission is plotted as a function of the potential strength for a double-barrier structure (red solid line) and for a single-barrier structure (blue dashed line). When the potential strength is small, the perfect

transmission occurs with $T = 1$ featuring the Klein paradox. With the potential height increased, the maximum transmission diminishes when the quasiparticle states in the barriers regions should be described by the Schrödinger equation and the tunneling is not the Klein-type any more. From Fig. 4, it can be seen that the approximate upper threshhold of the Dirac equation is less than 300 meV in graphene. The periodic resonance peaks result from the resonance effect in the barriers. In the barriers, the resonance condition is $E - U = \varepsilon_{\pm}$. So as the potential height increases, the transmission oscillates periodically.

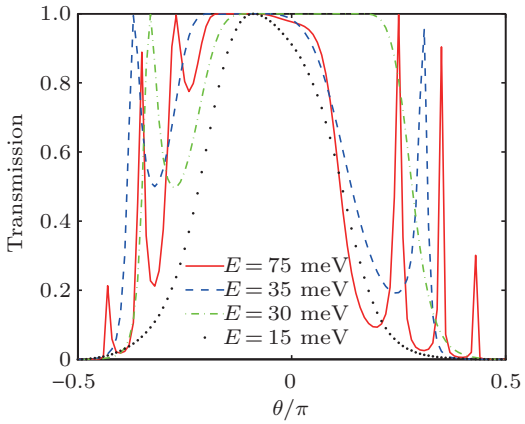


Fig. 3. (color online) Transmission probability as a function of the incident angle for different Fermi energies. Other parameters are $U = 1500$ meV, $N_1 = N_2 = 234$ and $M = 468$ (100 nm).

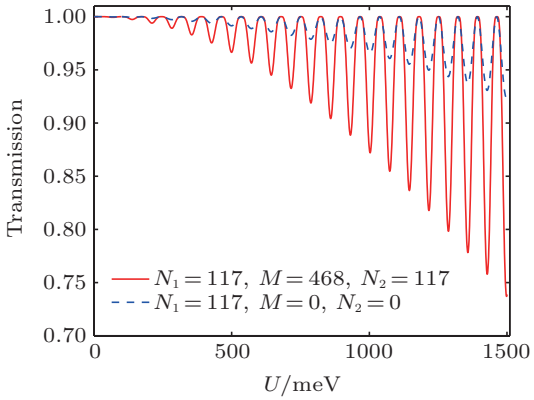


Fig. 4. (color online) Transmission probability as a function of the potential strength. The Fermi energy is $E = 100$ meV.

In Fig. 5, we plot an (N, M) contour of the transmission T in the normal incidence. The roughness of the contour edges is due to the discreteness in N and M, which makes sense only with integer values. It naturally recovers smoothness in its equivalent continuous model. As seen, the transmission oscillates as a function of the width N of the barrier regions with a period. This is the resonance effect in the barriers. We can obtain resonant peaks $N = [\pi(2n+1)/\kappa - 1]/2$, $n = 1, 2, \ldots, N$ from Eq. (8), where $\kappa \approx \pm(E - U)$. The T as a function of the width M of the middle region is also periodic due to the resonance effect in the middle region. The separation of resonant peaks of N is shorter that of M because of the potential U. In addition, when $N = 0$, the transmission is perfect because there are no barriers in the system.

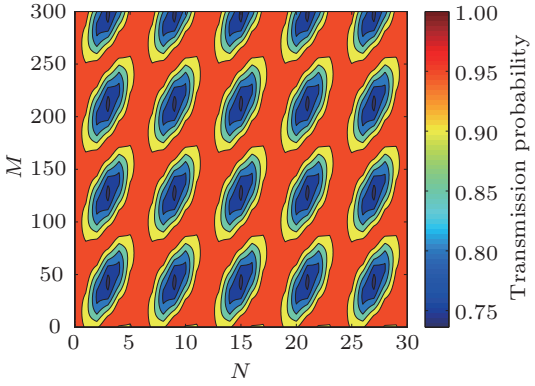


Fig. 5. (color online) Contour plot of the transmission probability. The parameters are $E = 100$ meV, $U = 1500$ meV and $N_1 = N_2 = N$.

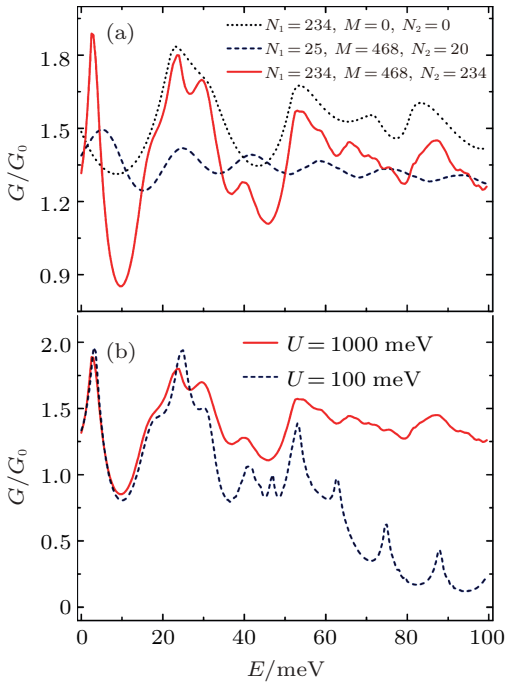


Fig. 6. (color online) Conductance as a function of the Fermi energy.

In Fig. 6, we plot the ballistic conductance as a function of the Fermi energy for different structure parameters. In Fig. 6(a), the black dotted, blue dashed and red solid lines correspond to the barriers and middle regions with $(N_1, M, N_2) = (234, 0, 0)$, $(25, 468, 20)$ and $(234, 468, 234)$, respectively. The parameter used in the calculation is $U = 1000$ meV. The resonance peaks of conductance result from the incident-angle averaged resonance effect of the barriers, that of the middle region and the hybridization between them. The resonant peaks are not equidistant because of the integral of all incident angles. In Fig. 6(b), the red solid and blue dashed lines correspond to the potentials with $U = 1000$ meV and $U = 100$ meV, respectively. Other parameters are $N_1 = N_2 = 234$ and $M = 468$. We can find that the conductances between them are similar. So the resonance effect has a significant influence on the

tunneling conductance even in the low energy. Actually, the Klein tunneling plays an important role in the transmission of normal incidence. For other incident angles, the transmission is a combined effect of the Klein paradox and the resonance effect. Another feature is that the high-barrier conductance at larger Fermi energies can be significantly larger than that of small barriers. In the former case, more resonant levels contribute to the conductance as the Fermi energy increases.

4. Summary

Based on the tight-binding approximation, we have investigated the resonant tunneling properties through double-barrier structures on graphene. The resonant transmission as a function of the Fermi energy, the incident angle, the potential strength, the widths of the barriers and the middle regions was calculated and the influence of the resonant tunneling to the conductance was discussed. It was shown that the resonance effect in this system includes the resonance in the barriers, the resonance in the middle region and the hybridization between them and that the resonant peaks are equidistant in the normal incidence. Compared to the low barriers, the conductance of high-barrier structures can be significantly increased due to the contribution from more resonant levels.

References

[1] Novoselov K S, Geim A K, Morozov S V, Jiang D, Zhang Y, Dubonos S V, Grigorieva I V and Firsov A A 2004 *Science* **306** 666
[2] Castro Neto A H, Guinea F, Peres N M R, Novoselov K S and Geim A K 2009 *Rev. Mod. Phys.* **81** 109
[3] Sarma S D, Adam S, Hwang E H and Rossi E 2011 *Rev. Mod. Phys.* **83** 407
[4] Katsnelson M I, Novoselov K S and Geim A K 2006 *Nat. Phys.* **2** 620
[5] Tworzydło J, Trauzettel B, Titov M, Rycerz A and Beenakker C W J 2006 *Phys. Rev. Lett.* **96** 246802
[6] Zhang Y B, Tan Y W, Stormer H L and Kim P 2005 *Nature* **438** 201
[7] Nomura K and MacDonald A H 2006 *Phys. Rev. Lett.* **96** 256602
[8] Brey L and Fertig H A 2006 *Phys. Rev. B* **73** 195408
[9] Tworzydło J, Trauzettel B, Titov M, Rycerz A and Beenakker C W J 2006 *Phys. Rev. Lett.* **96** 246802
[10] Zhu R and Guo Y 2007 *Appl. Phys. Lett.* **91** 252113
[11] DiCarlo L, Williams J R, Zhang Y M, McClure D T and Marcus C M 2008 *Phys. Rev. Lett.* **100** 156801
[12] Zhu R and Chen H 2009 *Appl. Phys. Lett.* **95** 122111
[13] Zhu R and Lai M L 2011 *J. Phys.: Condens. Matter* **23** 455302
[14] Prada E, San-Jose P and Schomerus H 2009 *Phys. Rev. B* **80** 245414
[15] Beenakker C W J 2006 *Phys. Rev. Lett.* **97** 067007
[16] Beenakker C W J 2008 *Rev. Mod. Phys.* **80** 1337
[17] Cheng S G, Xing Y, Wang J and Sun Q F 2009 *Phys. Rev. Lett.* **103** 167003
[18] Cheng S G, Zhang H and Sun Q F 2011 *Phys. Rev. B* **83** 235403
[19] Schelter J, Trauzettel B and Recher P 2012 *Phys. Rev. Lett.* **108** 106603
[20] Wang X R, Ouyang Y J, Li X L, Wang H L, Guo J and Dai H J 2008 *Phys. Rev. Lett.* **100** 206803
[21] Cayssol J, Huard B and Goldhaber-Gordon D 2009 *Phys. Rev. B* **79** 075428
[22] Zhao J, Zhang G Y and Shi D X 2013 *Chin. Phys. B* **22** 057701
[23] Wang X, Zhi L J and Müllen K 2008 *Nano Lett.* **8** 323
[24] Benjamin C and Pachos J K 2008 *Phys. Rev. B* **78** 235403
[25] Veldhorst M and Brinkman A 2010 *Phys. Rev. Lett.* **105** 107002
[26] Bai C X and Zhang X D 2007 *Phys. Rev. B* **76** 075430
[27] Pereira J M, Vasilopoulos Jr P and Peeters F M 2007 *Appl. Phys. Lett.* **90** 132122
[28] Ramezani Masir M, Vasilopoulos P, Matulis A and Peeters F M 2008 *Phys. Rev. B* **77** 235443
[29] Barbier M, Vasilopoulos P and Peeters F M 2009 *Phys. Rev. B* **80** 205415
[30] Wang L G and Zhu S Y 2010 *Phys. Rev. B* **81** 205444
[31] Guo X X, Liu D and Li Y X 2011 *Appl. Phys. Lett.* **98** 242101
[32] Reich S, Maultzsch J and Thomsen C 2002 *Phys. Rev. B* **66** 035412
[33] Deng W Y, Zhu R and Deng W J 2013 *Acta Phys. Sin.* **62** 067301 (in Chinese)
[34] Brey L and Fertig H A 2006 *Phys. Rev. B* **73** 235411
[35] Zheng H X, Wang Z F, Luo T, Shi Q W and Chen J 2007 *Phys. Rev. B* **75** 165414
[36] Landauer R 1957 *IBM J. Res. Dev.* **1** 223
[37] Büttiker M 1993 *J. Phys.: Condens. Matter* **5** 9361
[38] Christen T and Büttiker M 1996 *Phys. Rev. Lett.* **77** 143